

Membership determination in open clusters using the DBSCAN Clustering Algorithm

Mudasir Raja^a, Priya Hasan^{a,1}, Md Mahmudunnobe^c, Md Saifuddin^a, S N Hasan^a

^aMaulana Azad National Urdu University, Gachibowli, Hyderabad, 500 032, Telangana, India

^bInter-University Centre for Astronomy and Astrophysics, Post Bag 4 Ganeshkhind, Savitribai Phule Pune University Campus, Pune, 411 007, Maharashtra, India

^cWayne State University, 42 W Warren Ave, Detroit, 48202, MI, USA

Abstract

In this paper, we apply the machine learning clustering algorithm Density Based Spatial Clustering of Applications with Noise (DBSCAN) to study the membership of stars in twelve open clusters (NGC 2264, NGC 2682, NGC 2244, NGC 3293, NGC 6913, NGC 7142, IC 1805, NGC 6231, NGC 2243, NGC 6451, NGC 6005 and NGC 6583) based on Gaia DR3 Data. This sample of clusters spans a variety of parameters like age, metallicity, distance, extinction and a wide parameter space in proper motions and parallaxes. We obtain reliable cluster members using DBSCAN as faint as $G \sim 20$ mag and also in the outer regions of clusters. With our revised membership list, we plot color-magnitude diagrams and we obtain cluster parameters for our sample using ASteCA and compare it with the catalog values. We also validate our membership sample by spectroscopic data from APOGEE and GALAH for the available data. This paper demonstrates the effectiveness of DBSCAN in membership determination of clusters.

Keywords: (Galaxy:) open clusters and associations: general, individual: – (stars:) Hertzsprung–Russell and color-magnitude diagrams–machine learning: –DBSCAN

1. Introduction

Star clusters are the fundamental components of galaxies and play a vital role in understanding the formation and evolution of stars and galaxies (Janes and Phelps, 1994; Friel, 1995; Krumholz et al., 2019). An open cluster is a stellar system which is gravitationally bound and is made up of tens to thousands of stars and present an irregular and a loosely bound structure. Stars in a cluster are born from the same molecular cloud, at about the same time and hence they approximately are of the same chemical composition, same age and at the same distance. Most of the open clusters are located close to the Galactic plane and thus serve as excellent tracers of the recent formation history of the Galactic disc (Friel, 1995; Chen et al., 2003; Jacobson et al., 2016). Gaia DR3 (Prusti et al., 2016; Gaia Collaboration et al., 2017; Brown et al., 2021; Hasan, 2021; Collaboration et al., 2022) includes precise astrometry at the sub-milliarcsecond level and broad band photometry for a total of 1.8 billion objects based on 34 months of satellite data.

Previously, due to non-availability of extensive data on stars, many researchers studied specific regions (which often contained a small central region of an open star cluster), and employed membership determination methods that had limited application. The popular method for member determination of open clusters was the use of proper-motion data by the Vasilevskis-Sanders method (also called the VS method) proposed by Vasilevskis et al. (1958) which was improved by Sanders (1971). Zhao and He (1990) proposed an improved scheme to enable use of the VS method with the proper motion data of unequal inaccuracies. Other methods include (Cabrera-Cano and Alfaro, 1990; Galadi-Enriquez et al., 1998; Castro-Ginard et al., 2018). Photometric methods have also been used for membership determi-

nation (Hasan and Hasan, 2011).

Machine Learning (ML) provides improved methods of membership determination. Random Forest (RF) is a supervised classification method and was applied to the Gaia DR2 data in (Gao, 2018; Mahmudunnobe et al., 2021). Gaussian Mixture Modeling (GMM) was also explored by us Mahmudunnobe et al. (2024). Cantat-Gaudin et al. (2020) obtained reliable parameters for 1867 clusters by training an artificial neural network to estimate parameters from the Gaia DR2 photometry of cluster members and their mean parallax. Gao (2014) proposed to use a classical algorithm in the data mining—Density-Based Spatial Clustering of Applications with Noise (DBSCAN) clustering algorithm (Ester et al., 1996a) for the determination of members in open star clusters using the fact that cluster stars would be ‘clustered’ not only spatially, but also in parameter space. By using the 3D kinematic data (two-dimensional proper motion and radial velocity) of 1046 stars Gao (2014) determined members of NGC 188 and validated it by plotting the color-magnitude diagram. Castro-Ginard et al. (2018) used DBSCAN to find clusters in the Gaia DR2 data coupled with a supervised learning method such as an artificial neural network (ANN) to distinguish between real OCs and statistical clusters in an automated method. Shou-kun et al. (2019) used the DBSCAN clustering algorithm for the detection of nearby open clusters based on Gaia DR2 within 100 pc of the Sun. Castro-Ginard et al. (2020) used DBSCAN to blindly search for these overdensities in Gaia DR2 and then applied a deep learning artificial neural network trained on colour-magnitude diagrams to identify isochrone patterns in these overdensities, and confirm them as open clusters. Castro-Ginard et al. (2022) aimed to complete the open cluster census in the Milky Way

with the detection of new stellar groups in the Galactic disc using an OCfinder method. He et al. (2021) used Gaia DR2 to blindly search for open star clusters in the Milky Way within the Galactic latitude range of $b < 20^{\circ}$ using an unsupervised machine learning method. He et al. (2022) searched Gaia EDR3 for nearby (parallax > 0.8 mas) all-sky regions, to find 886 star clusters, of which 270 candidates were new. He et al. (2023) and earlier references by the authors, used DBSCAN algorithm to identify clusters on fainter and more distant stars.

The DBSCAN algorithm assumes an average density of stars in the region. In the case of regions that are small, the average is a good approximation compared to wider regions of the sky, where the density is not constant. In the case of wider searches, HDBSCAN proves more effective since it applies variable densities as used by Hunt and Reffert (2021); Hunt and Reffert (2023).

In an earlier work, we used DBSCAN, OPTICS and HDBSCAN to identify YSOs in Gaia data to study their distribution and kinematics in the Serpens Cloud Hasan et al. (2023).

As an extension of our exploration of different algorithms of membership determination (Mahmudunnobe et al., 2021, 2024; Hasan et al., 2023), in this paper, we shall focus on DBSCAN which is an unsupervised density based clustering technique that can identify clusters of non-spherical shapes and hence is highly suitable for open clusters in smaller regions of approximately constant densities. We use DBSCAN for membership determination using Gaia DR3 data (Gaia Collaboration et al., 2023) for a sample of twelve clusters. We provide the code for use by the community and queries can be addressed to PH¹

1.1. Epsilon and MinPts

The paper is structured as follows: Section 1 gives a brief introduction and a description of the problem. Section 2 describes the data and sample selection. Section 3 describes the DBSCAN Method. Section 4 describes the DBSCAN results. Section 5 describes the APOGEE and GALAH data. Section 6 presents ASteCA results and Section 7 is the Discussions and Conclusions part of our paper.

2. Cluster Sample

In this section we determine the membership of twelve open clusters: NGC 2264, NGC 2682, NGC 2244, NGC 3293, NGC 6913, NGC 7142, IC 1805, NGC 6231, NGC 2243, NGC 6451, NGC 6005 and NGC 6583.

These clusters have distances ranging from 707 pc to 3719 pc. The basic parameters of the selected clusters are given in Table 1 which shows the coordinates of these clusters (α and δ), the angular diameter ($r50$), the radius that contains half the number of members from the same reference, the logarithm of age $\log t$, the extinction A_V , the distance to the cluster in parsecs is d

¹The code used for a sample cluster is available at https://github.com/priyahasan/ML/blob/master/DBSCAN_6913.ipynb

Table 1: Basic cluster parameters (Cantat-Gaudin and Anders, 2020)

Cluster	α (deg)	δ (deg)	$r50$ (deg)	$\log t$	A_V mag	d (pc)	GC (pc)
NGC 2264	100.2	9.8	0.072	7.44	0.79	707	8995
NGC 2682	132.85	11.8	0.166	9.63	0.07	899	8964
NGC 2244	98.05	4.9	0.232	7.1	1.46	1478	9686
NGC 3293	157.97	-58.23	0.066	7.01	0.9	2710	8034
NGC 6913	305.9	38.48	0.106	7.34	1.8	1608	8126
NGC 7142	326.29	65.78	0.102	9.49	1.16	2406	9255
IC 1805	38.21	61.47	0.11	6.88	2.22	1964	9821
NGC 6231	253.545	-41.812	0.15	7.14	1.07	1475	6938
NGC 2243	97.4	-31.28	0.046	9.64	0.02	3719	10584
NGC 6451	267.675	-30.206	0.078	7.41	2.2	2777.0	5563
NGC 6005	238.955	-57.439	0.057	9.1	1.42	2383.0	6510
NGC 6583	273.962	-22.143	0.046	9.08	1.52	2053.0	6323

and GC is the galactocentric distance in parsecs from (Cantat-Gaudin and Anders, 2020). The WISE images of the cluster sample are shown in Fig. 1. We choose to present these as WISE images are in the infrared and can give an idea of the reddening (gas and dust) in the cluster sample. This is a good indicator of the possible obscured stars since Gaia observes in the optical.

3. DBSCAN Analysis

For each cluster, we used a search radius which was double the maximum radius found in Cantat-Gaudin and Anders (2020), where the maximum radius is defined as the distance of the farthest members from the center. Henceforth Cantat-Gaudin and Anders (2020) members will be referred to as CG members. The stars extracted from the Gaia archive were filtered to ensure quality check where the parallax is greater than zero, parallax over error was greater than or equal to 3 and the errors in proper motion in ra and dec were less than 1. Also to ensure single stars, the RUWE factor was taken to be less than 1.4.

Before applying DBSCAN, we first normalized the data to ensure that the difference in the range of the variables does not influence the analysis. The data was normalized using the Z-score normalization, where we used median instead of mean,

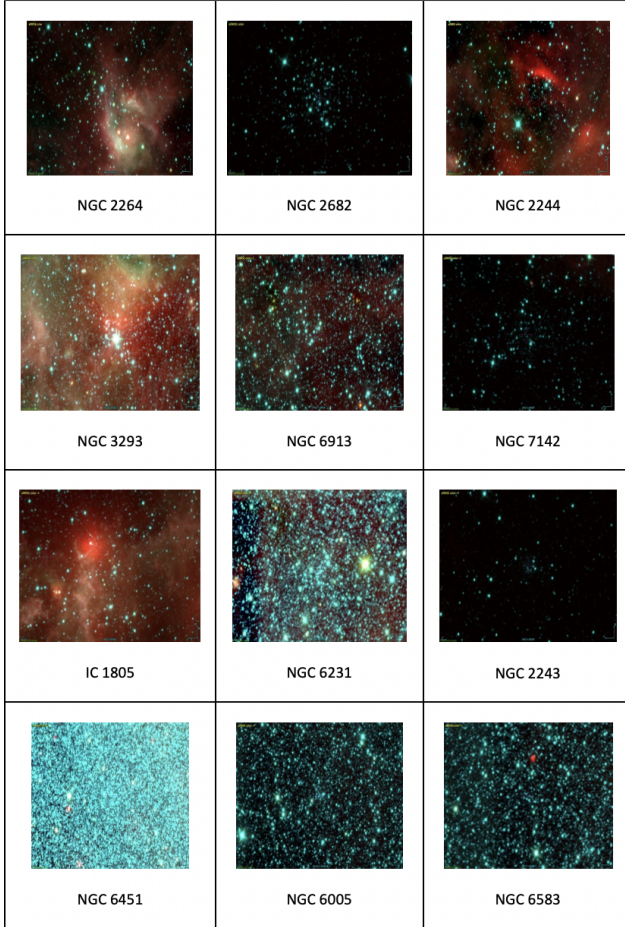


Figure 1: WISE images of the cluster sample: NGC 2264, NGC 2682, NGC 2244, NGC 3293, NGC 6913, NGC 7142, IC 1805, NGC 6231, NGC 2243, NGC 6451, NGC 6005 and NGC 6583. In all images, North is up, East is left. Field of View: '34.2 X 20.6'

since mean is affected strongly by outliers. We therefore subtracted the median of the feature from each value, and then divided it by the standard deviation, resulting in values that have a median of 0 and a standard deviation of 1.

The DBSCAN model defines groups as dense regions in parameter space that are separated by the sparser regions. It has the advantage over GMM of identifying non-symmetric regions. As the data was queried in RA and Dec, the DBSCAN was run for pmra, pmdec and parallax. *MinPts* represents the minimum number of points required to form a group, whereas epsilon (ϵ) is the radius around each point where DBSCAN searches for neighboring points. DBSCAN model starts with a random point and finds all the points within its ϵ -neighborhood. The distance in parameter space between two points i and j is defined as:

$$d_{ij} = \sqrt{\sum_{n=1}^k (x_{i,n} - x_{j,n})^2}$$

where k is the number of dimensions of our data. If a point has atleast *MinPts* in its ϵ -neighborhood, it is considered a core point. If the number of neighbors is less than *MinPts*, but the point itself is a neighbor of a core point, it is considered a border point. The points which are neither core nor border, are labeled as noise points. The neighboring core and border points form a cluster. After running DBSCAN, we get one or more clusters of stars along with noise points. Finally, we chose the DBSCAN cluster with the larger number of stars as the members of the cluster and the noise points as the field stars. We may get one or more clusters, but the user has to decide which is the cluster in consideration.

3.1. Model Parameter Optimization

Like any machine learning algorithm, the model parameters ϵ and *Minpts* directly affect the clustering effectiveness and therefore we need to optimize these parameters to get the most efficient model. Increasing *Minpts* makes the algorithm more conservative, as it requires denser regions to form a group, potentially ignoring smaller, less dense groups. Similarly smaller ϵ results in compact groups, while a larger ϵ may merge different groups and/or noise.

To get the most optimal value for these two parameters, we used elbow plots or k -dist plots as used by Shou-kun et al. (2019); Ester et al. (1996b) and mean nearest neighbors were found as in Gao (2014). For our analysis, we used a combination of k -dist plot, Mean Nearest Neighbour (*MNN*), Modified Silhouette Score (*MSS*) and number of retrieved members to optimize ϵ and *MinPts* which are discussed below.

3.1.1. k -dist Plots:

Using this principle, if we find a clear elbow point in the k -th nearest neighbor plot (k -dist plot), then we can use $k+1$ as our *MinPts* and the distance at the boundary (i.e., the elbow point) as our ϵ . This method was suggested by Ester et al. (1996b) and used by Shou-kun et al. (2019) to get the members of the Hyades open cluster.

One issue with k -dist plot is that it requires a visual inspection of the plot and thus can be subjective. Especially when we have a large dataset (like Gaia) and a larger fraction of field stars, it becomes more uncertain to pinpoint an exact elbow point from the plot. Due to this reason, we did not use the k -dist plot as our final metric to choose optimal parameters. However, we used k -dist plot to have an idea of possible ranges of $MinPts$ and ϵ , outside of which the k -dist plots clearly do not show any boundary. Then we run the DBSCAN model for all combinations of $MinPts$ and ϵ in this range and measure their performance using MNN and MSS metrics.

3.1.2. Mean Nearest Neighbour (MNN) Distance

MNN distance is defined as the mean distance of the nearest neighbor of each star in the group. As the clusters are compact and members are close to each other in the parameter space, their MNN distance would be small for clusters. We finalized the value of ϵ and $MinPts$ using the elbow plots as shown for NGC 6005 in Fig.2, where we get low values for MNN distance. We also determined the number of retrieved members for different pairs of ϵ and $MinPts$. When the MNN distance for two or more pairs is very similar, we chose the one with the highest number of members. For all twelve clusters, we found different optimal values of ϵ and $MinPts$ as reported in Table 2. This was used in the analysis.

3.2. Modified Silhouette Score (MSS)

The Silhouette Score is a metric used to calculate the performance of a given clustering technique and validate the clustering algorithm. When using the silhouette approach, each point's silhouette coefficients are calculated, which indicates how much a point resembles its own cluster in relation to other clusters by offering a concise graphic illustration of how accurately each cluster has been identified.

The silhouette score is a representation of how far away an object is from other clusters (separation) compared to its own cluster (cohesion). A high value means the object is well-matched to its own cluster and poorly matched to neighboring clusters. The value of the silhouette runs between $[1, -1]$. The clustering process is useful if the majority of the items have high values. A clustering setup may have too many or too few clusters if a large number of points have low or negative values. The silhouette coefficient for the sample point is defined as,

$$s = \frac{b - a}{\max(a, b)}$$

where a is the mean distance between a sample and all other points in the same class and b is the mean distance between the sample and all other points in the next class.

The problem in this metric is that the silhouette score assumes that all clusters are dense and well separated, which is not true in the case of star clusters. We have a member set, that is compact and dense in all the feature-variable spaces. But our field stars are random and uniform in all feature spaces and is mixed with the member set in feature space. Even when we have a good separation of member and field stars, for a member

star the value of b would be close to the value of a , as the field stars are uniformly found all around the member set. Hence, the silhouette score will be close to 0.

We shall use another property of our sample in this case. The standard deviation (σ) of the members would be small due to the cluster's compact nature. On the other hand, the field stars are dispersed evenly, which means that their σ ought to be high. Therefore, in our case, σ as a metric may be more helpful than the comparison of the distance between clusters. Therefore, a new metric is proposed for evaluating performance for clustering by an unsupervised model by making certain adjustments to the silhouette score. This newly proposed metric is named as the Modified Silhouette Score (MSS) and is denoted by

$$MSS = \frac{1}{k} \sum_{i=1}^k \frac{(\sigma_{i,field} - \sigma_{i,member})}{\max(\sigma_{i,field}, \sigma_{i,member})} \quad (1)$$

where k is the total number of features and $\sigma_{i,field}$ and $\sigma_{i,member}$ denote the σ of the feature i for field stars and members respectively (Mahmudunnobe et al., 2024).

We would expect that a well-performed model would show the members to be distributed normally with a very small σ and the field stars to be uniformly distributed, i.e., with a high σ .

In this case, we would have $\sigma_{field} \gg \sigma_{member}$, therefore the numerator will be $\sigma_{field} - \sigma_{i,member} \approx \sigma_{i,field}$. This will result in an MSS value very close to 1. On the other hand, for a poor performance model, the member and field stars both will have a similar random distributions. Thus, the numerator will be close to 0, resulting in an MSS value around 0. One special case is when the predicted field star group shows a stronger normal distribution (thus having low σ), but the predicted member group is distributed randomly (a larger σ). In this case, the numerator will be $\sigma_{field} - \sigma_{i,member} \approx -\sigma_{i,member}$ and the MSS value will be around -1. So, a strong negative MSS value will likely indicate that the model was able to distinguish well between member and field stars, but it mislabeled the groups. The predicted member group is the field star group and vice-versa.

Figure 2 shows the plots of ϵ and $MinPts$ for NGC 6005. Here, we choose $\epsilon (= 0.06)$ that gives a small MNN distance as this is a cluster. We also note that with $\epsilon (= 0.06)$, our MSS value exceeds 0.9. Further in the third plot, we notice the elbow first appearing for $MinPts = 30 - 40$. Hence we take $MinPts = 35$.

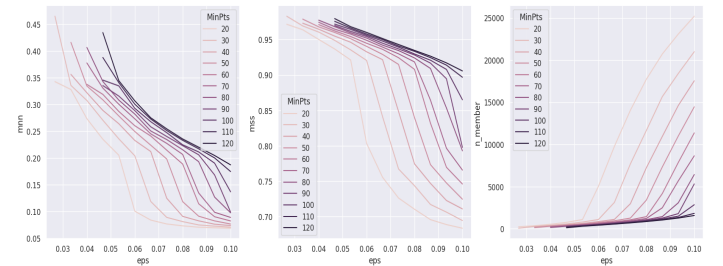


Figure 2: Parameters ϵ and $MinPts$ optimization using the MNN distance and no of members for NGC 6005.

4. DBSCAN Results

Table 2 describes the values of ϵ and $MinPts$ selected and the parallax obtained for our sample of clusters.

Table 2: DBSCAN Parameters of the sample data

Cluster	RA deg	DEC deg	Epsilon ϵ	$MinPts$	Parallax mas
NGC 2264	100.2	9.8	0.06	20	1.38 ± 0.08
NGC 2682	132.8	11.8	0.06	35	1.15 ± 0.07
NGC 2244	98.0	4.9	0.065	25	0.66 ± 0.09
NGC 3293	80.7	33.4	0.065	25	0.39 ± 0.05
NGC 6913	305.9	38.5	0.05	40	0.56 ± 0.05
NGC 7142	326.3	65.8	0.06	20	0.40 ± 0.06
IC 1805	38.2	61.5	0.05	30	0.41 ± 0.06
NGC 6231	235.5	-41.8	0.04	20	0.60 ± 0.07
NGC 2243	97.4	-31.3	0.06	15	0.25 ± 0.05
NGC 6451	267.675	-30.206	0.07	100	0.35 ± 0.06
NGC 6005	238.955	-57.439	0.07	100	0.38 ± 0.05
NGC 6583	273.962	-22.143	0.06	50	0.41 ± 0.05

The results for memberships obtained after using DBSCAN algorithm are shown in Table 3 and compared with the CG members.

Figures 3 to 14 show plots of the revised membership in our sample of clusters where CG(orange) and DBSCAN (green). The upper left plot shows the histogram of the parallax distribution of the CG members and the members found by our sample. The upper middle plot and the upper right plots show the histogram of the proper motion distributions of $pmra$ and $pmdec$. Our sample has a narrower distribution of parallax and proper motions with a smaller standard deviation as we have used DR3 data, while CG is based on DR2 data. The lower plots show the sky plot (lower left), the proper motion plot (lower middle) and the color-magnitude diagram (lower right) of the CG(orange) and DBSCAN (green) members. The plot shows we have explored the outer regions of the clusters and have found fainter members down to 20^m . Noormohammadi et al. (2023) used DBSCAN and GMM to find members of 12 open clusters. Of these we have in common two clusters: NGC 2682 (M67) and NGC 2243. And our values are in good agreement as shown in Table 4.

Table 3: Performance of DBSCAN for sample clusters

Cluster	MNN	MSS	Member D	Member CG	Ratio D/CG	Sample after filters
NGC 2264	0.33	0.94	325	186	1.75	4829
NGC 2682	0.23	0.95	1222	848	1.44	2576
NGC 2244	0.19	0.91	1803	1701	1.05	6530
NGC 3293	0.2	0.94	1027	657	2.23	27552
NGC 6913	0.25	0.95	824	170	4.85	13660
NGC 7142	0.23	0.93	813	539	1.50	9820
IC 1805	0.18	0.92	1252	456	2.74	9472
NGC 6231	0.17	0.92	2032	1560	1.29	24895
NGC 2243	0.29	0.96	548	531	1.03	5380
NGC 6451	0.20	0.93	1560	1171	1.33	50422
NGC 6005	0.21	0.92	1072	708	1.5	50570
NGC 6583	0.3	0.94	455	364	1.25	47821

In Fig. 6 for NGC 3293, it is visible that even Cantat-Gaudin data has a hint of a double peak in $pmra$. In our case, this peak has got more enhanced. There is definitely some sub-structure in NGC 3293 in the velocity space that needs to be explored in detail.

5. Spectroscopic Data: APOGEE and GALAH

As the member stars are born from the same molecular cloud, their chemical abundances should be similar. We compared the chemical abundances of the DBSCAN members and the members found by Cantat-Gaudin et al. (2018) using APOGEE and GALAH data, where available. Apache Point Observatory Galactic Evolution Experiment (APOGEE) is a large scale, stellar spectroscopic survey which is conducted in the near infrared (IR) region of the electromagnetic spectrum. APOGEE (Majewski et al., 2017) observations provide $R \sim 22,500$ spectra in the infrared H-band, $1.5 - 1.7 \mu m$, as part of the third and fourth phases of the Sloan Digital Sky Survey (Eisenstein et al., 2011; Blanton et al., 2017).

Figures 15 show the chemical abundances of members of NGC 2264 from APOGEE. The upper plots shows members found by Cantat-Gaudin et al. (2018) and the lower ones are our results. The rest of the plots are in Appendix Appendix A.

The Galactic Archaeology with HERMES (GALAH) is a high resolution, ground-based spectroscopic survey. It is car-

Table 4: Comparison of DBSCAN results with Noormohammadi et al. (2023)(NM)

Cluster	Parallax mas	pmra mas yr ⁻¹	pmdec mas yr ⁻¹	distance pc
NGC 2682				
Ours	1.14±0.06	-10.96±0.2	-2.90±0.19	877.1
NM	1.15±0.09	-10.96±0.09	-2.90±0.07	864.3
NGC 2243				
Ours	0.25±0.06	-1.25 ± 0.09	5.49± 0.05	4000
NM	0.23 ± 0.08	-1.26±0.09	5.50±0.09	3660.6

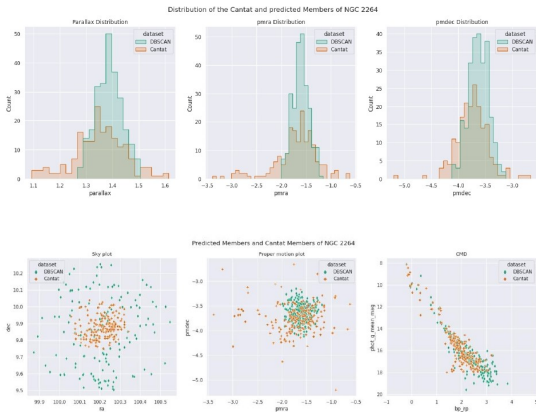


Figure 3: Revised members of NGC 2264 CG(orange) and DBSCAN (green).

ried out using the Anglo-Australian Telescope’s Two Degree Field (2dF) of view and the High Efficiency and Resolution Multi-Element Spectrograph (HERMES) (Barden et al., 2010; Heijmans et al., 2012; Sheinis et al., 2015). The HERMES spectrograph gives a high resolution ($R \sim 28000$) spectra for 392 stars in four passbands. Table 5 shows the number of stars that matched with (Cantat-Gaudin et al., 2018) and DBSCAN members from APOGEE and GALAH surveys.

The figures show a good agreement in chemical abundances obtained by (Cantat-Gaudin et al., 2018) and DBSCAN members obtained by us.

Figures 16 shows the chemical abundances of members of NGC 2682 from GALAH. The upper plot shows members found by (Cantat-Gaudin et al., 2018) and the lower one is our result. The rest of the plots are in Appendix Appendix A.

6. ASteCA Results

ASteCA Perren et al. (2015) is a software package that does an automated analysis of photometric data of star clusters. Input parameter and data files are provided to run the code in a specified format that gives an output of all necessary cluster parameters and plots. ASteCA performs an exhaustive analysis

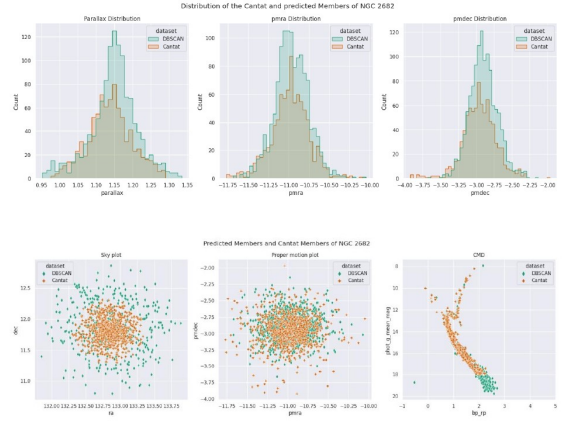


Figure 4: Revised members of NGC 2682 CG(orange) and DBSCAN (green).

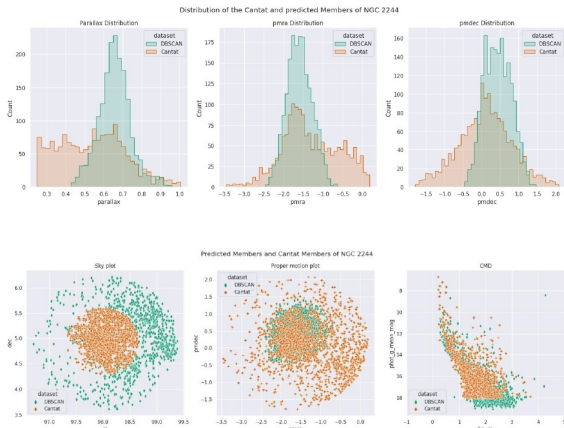


Figure 5: Revised members of NGC 2244 CG(orange) and DBSCAN (green).

by using both spatial and photometric data. The structural parameters of a star cluster, such as its exact centre location and radius value, are derived from positional data, while the remaining functions require an observed magnitude and colour.

Table 6 shows the ASteCA parameters of some of our sample clusters and found that they compare well with the Cantat-Gaudin and Anders (2020) values. Figures 17 to B.37 show ASteCA plots and CMDs of the revised members that we obtained after running DBSCAN clustering algorithm on our sample.

We have used ASteCA to find parameters of the clusters studied using the revised membership data. Figures. 17 - 18 show plots for NGC 2682. The rest of the plots are in the Appendix Appendix B.

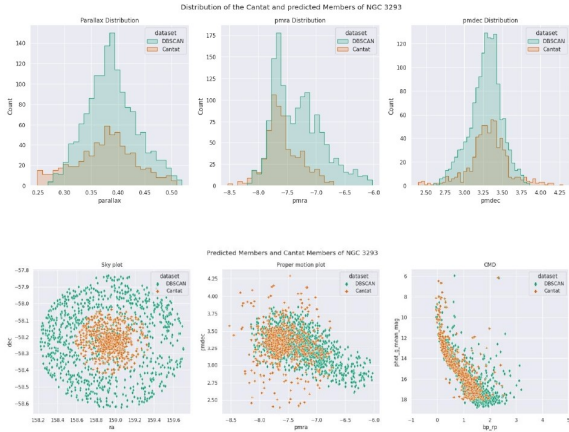


Figure 6: Revised members of NGC 3293 CG(orange) and DBSCAN (green).

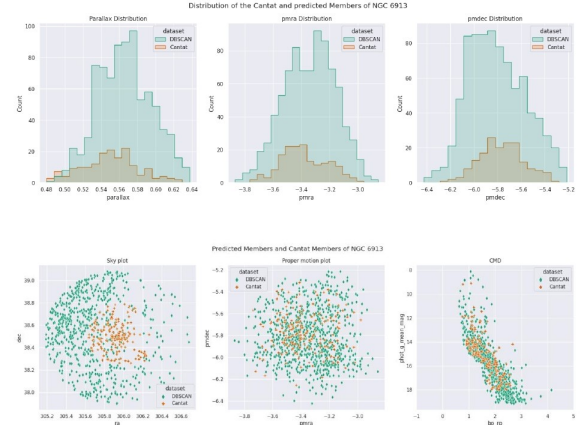


Figure 7: Revised members of NGC 6913 CG(orange) and DBSCAN (green).

7. Conclusion and Discussion

DBSCAN is an unsupervised method used to identify clusters in the data. In this work, we used the DBSCAN algorithm to find the membership of stars in twelve open clusters (NGC 2264, NGC 2682, NGC 2244, NGC 3293, NGC 6913, NGC 7142, IC 1805, NGC 6231, NGC 2243, NGC 6451, NGC 6005 and NGC 6583) based on Gaia DR3 Data. Since DBSCAN requires no prior knowledge about the clusters (Ester et al., 1996b), it provides an unbiased method to identify the cluster members, compared to our earlier work using the supervised method of Random Forest (Mahmudunnobe et al., 2021). We made use of the elbow method using k -dist graphs as suggested by (Shou-kun et al., 2019), and the MNN and MSS metrics to find the optimal range of values of ϵ and $MinPts$. The revised list of members obtained by us increased the number upto 4.85 times and found fainter members in the outer regions of clusters.

We also compared the chemical abundances of our obtained members from APOGEE and GALAH and found an agreement with the chemical abundances of the members obtained by (Cantat-Gaudin et al., 2018). Table 3 shows the values of MNN , MSS and CG members and those we obtained. We also compare the values for cluster parameters obtained by us using ASteCA with the values obtained by (Cantat-Gaudin et al., 2018). We find our method to be very effective even for inner disk clusters with high field star contamination as well as for clusters of varying ages, distances and locations in the Galaxy.

This revised sample of cluster members can be used to find the Initial Mass Function (IMF), mass segregation, variable stars and to study features of the color magnitude diagram like gaps Hasan (2023) and many more detailed studies of star clusters. We plan to explore these in our future work.

8. Acknowledgements

This work has made use of data from the European Space Agency (ESA) mission *Gaia* (<https://www.cosmos.esa.int/gaia>), processed by the *Gaia* Data Processing and Analysis Consortium (DPAC, <https://www.cosmos.esa.int/web/gaia/dpac/consortium>). Funding for the DPAC has been provided by national institutions, in particular the institutions participating in the *Gaia* Multilateral Agreement.

We would also like to thank our anonymous referee whose valuable comments helped improve the quality of this paper.

References

- Barden, S.C., Jones, D.J., Barnes, S.I., Heijmans, J., Heng, A., Knight, G., Orr, D.R., Smith, G.A., Churilov, V., Brzeski, J., et al., 2010. Hermes: revisions in the design for a high-resolution multi-element spectrograph for the aat, in: Ground-based and Airborne Instrumentation for Astronomy III, SPIE. pp. 140–158.
- Blanton, M.R., Bershady, M.A., Abolfathi, B., Albareti, F.D., Prieto, C.A., Almeida, A., Alonso-García, J., Anders, F., Anderson, S.F., Andrews, B., et al., 2017. Sloan digital sky survey iv: Mapping the milky way, nearby galaxies, and the distant universe. *The Astronomical Journal* 154, 28.
- Brown, A.G., Vallenari, A., Prusti, T., De Bruijne, J., Babusiaux, C., Biermann, M., Creevey, O., Evans, D., Eyer, L., Hutton, A., et al., 2021. Gaia early data release 3-summary of the contents and survey properties. *Astronomy & Astrophysics* 649, A1.
- Cabrera-Cano, J., Alfaro, E., 1990. A non-parametric approach to the membership problem in open clusters. *Astronomy and Astrophysics* 235, 94–102.
- Cantat-Gaudin, T., Anders, F., 2020. Clusters and mirages: Cataloguing stellar aggregates in the milky way. *Astronomy & Astrophysics* 633, A99.
- Cantat-Gaudin, T., Anders, F., Castro-Ginard, A., Jordi, C., Romero-Gómez, M., Soubiran, C., Casamiquela, L., Tarricq, Y., Moitinho, A., Vallenari, A., Bragaglia, A., Krone-Martins, A., Kounkel, M., 2020. Painting a portrait of the Galactic disc with its stellar clusters. *Astron. Astrophys.* 640, A1. doi:10.1051/0004-6361/202038192, arXiv:2004.07274.
- Cantat-Gaudin, T., Jordi, C., Vallenari, A., Bragaglia, A., Balaguer-Núñez, L., Soubiran, C., Bossini, D., Moitinho, A., Castro-Ginard, A., Krone-Martins, A., et al., 2018. A gaia dr2 view of the open cluster population in the milky way. *Astronomy & Astrophysics* 618, A93.
- Castro-Ginard, A., Jordi, C., Luri, X., Álvarez Cid-Fuentes, J., Casamiquela, L., Anders, F., Cantat-Gaudin, T., Monguió, M., Balaguer-Núñez, L., Solà,

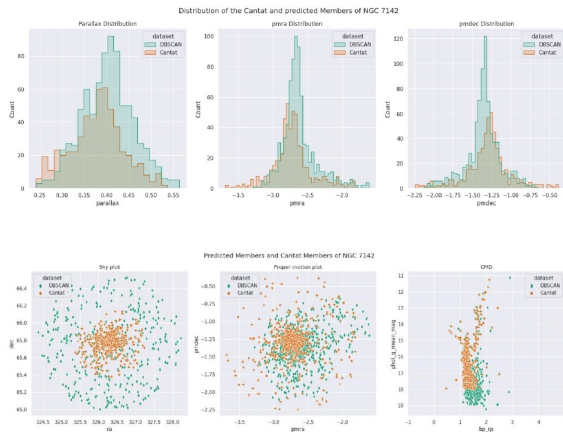


Figure 8: Revised members of NGC 7142 CG(orange) and DBSCAN (green).

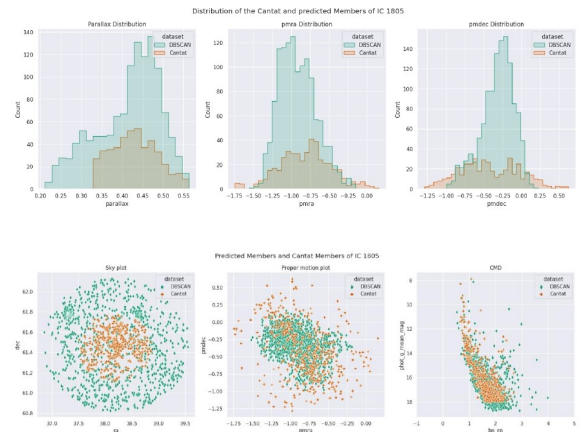


Figure 9: Revised members of IC 1805 CG(orange) and DBSCAN (green).

S., Badia, R.M., 2020. Hunting for open clusters in Gaia DR2: 582 new open clusters in the Galactic disc. *Astron. Astrophys.* 635, A45. doi:10.1051/0004-6361/201937386, arXiv:2001.07122.

Castro-Ginard, A., Jordi, C., Luri, X., Cantat-Gaudin, T., Carrasco, J.M., Casamiquela, L., Anders, F., Balaguer-Núñez, L., Badia, R.M., 2022. Hunting for open clusters in Gaia EDR3: 628 new open clusters found with OCfinder. *Astron. Astrophys.* 661, A118. doi:10.1051/0004-6361/202142568, arXiv:2111.01819.

Castro-Ginard, A., Jordi, C., Luri, X., Julbe, F., Morvan, M., Balaguer-Núñez, L., Cantat-Gaudin, T., 2018. A new method for unveiling open clusters in Gaia. New nearby open clusters confirmed by DR2. *Astron. Astrophys.* 618, A59. doi:10.1051/0004-6361/201833390, arXiv:1805.03045.

Castro-Ginard, A., Jordi, C., Luri, X., Julbe, F., Morvan, M., Balaguer-Núñez, L., Cantat-Gaudin, T., 2018. A new method for unveiling open clusters in Gaia-new nearby open clusters confirmed by dr2. *Astronomy & Astrophysics* 618, A59.

Chen, L., Hou, J., Wang, J., 2003. On the galactic disk metallicity distribution from open clusters. i. new catalogs and abundance gradient. *The Astronomical Journal* 125, 1397.

Collaboration, G., Bailer-Jones, C., Teyssier, D., Delchambre, L., Ducourant, C., Garabato, D., Hatzidimitriou, D., Klioner, S., Rimoldini, L., Bellas-Velidis, I., et al., 2022. Gaia data release 3: The extragalactic content. *Astronomy & Astrophysics*.

Eisenstein, D.J., Weinberg, D.H., Agol, E., Aihara, H., Prieto, C.A., Anderson, S.F., Arns, J.A., Aubourg, É., Bailey, S., Balbinot, E., et al., 2011. Sdss-iii: Massive spectroscopic surveys of the distant universe, the milky way, and extra-solar planetary systems. *The Astronomical Journal* 142, 72.

Ester, M., Kriegel, H., Sander, J., Xu, X., Simoudis, E., Han, J., Fayyad, U., 1996a. Proc. 2nd int. conf. on knowledge discovery and data mining (kdd'96).

Ester, M., Kriegel, H.P., Sander, J., Xu, X., 1996b. Kdd-96 proceedings, in: Second International Conference on Knowledge Discovery and Data Mining.

Friel, E., 1995. The old open clusters of the milky way. *Annual Review of Astronomy and Astrophysics* 33, 381–414.

Gaia Collaboration, van Leeuwen, F., Vallenari, A., Jordi, C., Lindegren, L., Bastian, U., Prusti, T., de Bruijne, J., Brown, A., Babusiaux, C., et al., 2017. Gaia data release. *A&A* 601, A19.

Gaia Collaboration, et al., 2023. Gaia Data Release 3. Summary of the content and survey properties. *Astron. Astrophys.* 674, A1. doi:10.1051/0004-6361/202243940, arXiv:2208.00211.

Galadí-Enriquez, D., Jordi, C., Trullols, E., 1998. The overlapping open clusters ngc 1750 and ngc 1758. iii. cluster-field segregation and clusters physical parameters. *Astronomy and Astrophysics* 337, 125–140.

Gao, X., 2018. A machine-learning-based investigation of the open cluster m67. *The Astrophysical Journal* 869, 9.

Gao, X.H., 2014. Membership determination of open cluster ngc 188 based on the dbscan clustering algorithm. *Research in Astronomy and Astrophysics* 14, 159.

Hasan, P., 2021. Gaia: The 3d milky way mapper. arXiv:2106.05125.

Hasan, P., 2023. Gaps in the main-sequence of star cluster hertzsprung russell diagrams. arXiv:2310.17725.

Hasan, P., Hasan, S.N., 2011. Mass segregation in diverse environments. *Monthly Notices of the Royal Astronomical Society* 413, 2345–2357. URL: <https://doi.org/10.1111/j.1365-2966.2011.18305.x>, doi:10.1111/j.1365-2966.2011.18305.x.

Hasan, P., Raja, M., Saifuddin, M., Hasan, S.N., 2023. Enhanced YSO population in Serpens. *Journal of Astrophysics and Astronomy* 44, 41. doi:10.1007/s12036-023-09945-9, arXiv:2303.07752.

He, Z., Luo, Y., Wang, K., Ren, A., Peng, L., Cui, Q., Liu, X., Jiang, Q., 2023. Survey for Distant Stellar Aggregates in the Galactic Disk: Detecting 2000 Star Clusters and Candidates, along with the Dwarf Galaxy IC 10. *Astrophys. J. Suppl.* 267, 34. doi:10.3847/1538-4365/acd6fa, arXiv:2305.10269.

He, Z., Wang, K., Luo, Y., Li, J., Liu, X., Jiang, Q., 2022. A Blind All-sky Search for Star Clusters in Gaia EDR3: 886 Clusters within 1.2 kpc of the Sun. *Astrophys. J. Suppl.* 262, 7. doi:10.3847/1538-4365/ac7c17, arXiv:2206.12170.

He, Z.H., Xu, Y., Hao, C.J., Wu, Z.Y., Li, J.J., 2021. A catalogue of 74 new open clusters found in Gaia Data-Release 2. *Research in Astronomy and Astrophysics* 21, 093. doi:10.1088/1674-4527/21/4/93, arXiv:2010.14870.

Heijmans, J., Asplund, M., Barden, S., Birchall, M., Carollo, D., Bland-Hawthorn, J., Brzeski, J., Case, S., Churilov, V., Colless, M., et al., 2012. Integrating the hermes spectrograph for the aat, in: *Ground-based and Airborne Instrumentation for Astronomy IV*, SPIE. pp. 287–303.

Hunt, E.L., Reffert, S., 2021. Improving the open cluster census. *Astronomy and Astrophysics* 646, A104. URL: <https://doi.org/10.1051/0004-6361/202039341>, doi:10.1051/0004-6361/202039341.

Hunt, E.L., Reffert, S., 2023. Improving the open cluster census. II. An all-sky cluster catalogue with Gaia DR3. *Astron. Astrophys.* 673, A114. doi:10.1051/0004-6361/202346285, arXiv:2303.13424.

Jacobson, H.R., Friel, E., Jilková, L., Magrini, L., Bragaglia, A., Vallenari, A., Tosi, M., Randich, S., Donati, P., Cantat-Gaudin, T., et al., 2016. The Gaia-ESO survey: Probes of the inner disk abundance gradient. *Astronomy & Astrophysics* 591, A37.

Janes, K., Phelps, R., 1994. The galactic system of old star clusters: The development of the galactic disk. *The Astronomical Journal* 108, 1773–1785.

Krumholz, M.R., McKee, C.F., Bland-Hawthorn, J., 2019. Star clusters across

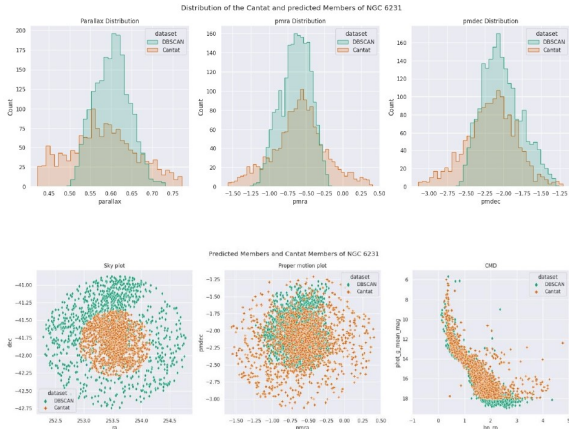


Figure 10: Revised members of NGC 6231CG(orange) and DBSCAN (green).

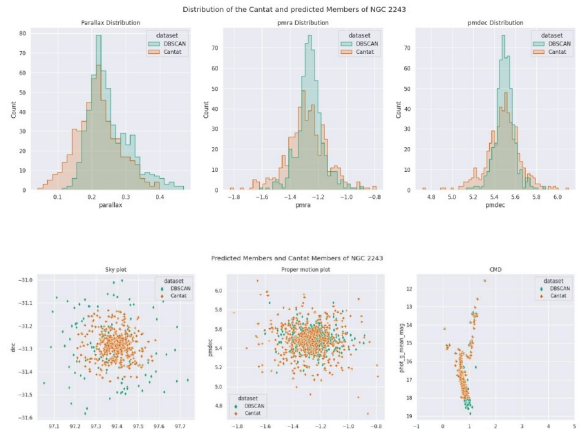


Figure 11: Revised members of NGC 2243 CG(orange) and DBSCAN (green).

cosmic time. *Annual Review of Astronomy and Astrophysics* 57, 227–303. URL: <https://doi.org/10.1146/annurev-astro-091918-104430>, doi:10.1146/annurev-astro-091918-104430, arXiv:<https://doi.org/10.1146/annurev-astro-091918-104430>.

Mahmudunnobe, M., Hasan, P., Raja, M., Hasan, S., 2021. Membership of stars in open clusters using random forest with gaia data. *The European Physical Journal Special Topics* 230, 2177–2191.

Mahmudunnobe, M., Hasan, P., Raja, M., Saifuddin, M., Hasan, S.N., 2024. Using gmm in open cluster membership: An insight. arXiv:2401.10802.

Majewski, S.R., Schiavon, R.P., Frinchaboy, P.M., Prieto, C.A., Barkhouser, R., Bizyaev, D., Blank, B., Brunner, S., Burton, A., Carrera, R., et al., 2017. The apache point observatory galactic evolution experiment (apogee). *The Astronomical Journal* 154, 94.

Noormohammadi, M., Khakian Ghomi, M., Hagi, H., 2023. The membership of stars, density profile, and mass segregation in open clusters using a new machine learning-based method. *Monthly Notices of the Royal Astronomical Society* 523, 3538–3554. URL: <https://doi.org/10.1093/mnras/stad1589>, doi:10.1093/mnras/stad1589, arXiv:<https://academic.oup.com/mnras/article-pdf/523/3/3538/50570039/stad1589.pdf>.

Perren, G.I., Vazquez, R.A., Piatti, A.E., 2015. Asteca: Automated stellar cluster analysis. *Astronomy & Astrophysics* 576, A6.

Prusti, T., De Bruijne, J., Brown, A.G., Vallenari, A., Babusiaux, C., Bailer-Jones, C., Bastian, U., Biermann, M., Evans, D.W., Eyer, L., et al., 2016. The gaia mission. *Astronomy & astrophysics* 595, A1.

Sanders, W., 1971. An improved method for computing membership probabilities in open clusters. *Astronomy and Astrophysics* 14, 226–232.

Sheinis, A., Anguiano, B., Asplund, M., Bacigalupo, C., Barden, S., Birchall, M., Bland-Hawthorn, J., Brzeski, J., Cannon, R., Carollo, D., et al., 2015. First light results from the high efficiency and resolution multi-element spectrograph at the anglo-australian telescope. *Journal of Astronomical Telescopes, Instruments, and Systems* 1, 035002–035002.

Shou-kun, X., Chao, W., Li-hua, Z., Xin-hua, G., 2019. Dbscan clustering algorithm for the detection of nearby open clusters based on gaia-dr2two. *Chinese Astronomy and Astrophysics* 43, 225–236.

Vasilevskis, S., Klemola, A., Preston, G., 1958. Relative proper motions of stars in the region of the open cluster ngc 6633. *The Astronomical Journal* 63, 387–395.

Zhao, J., He, Y., 1990. An improved method for membership determination of stellar clusters with proper motions with different accuracies. *Astronomy and Astrophysics* 237, 54–60.



Figure 12: Revised members of NGC 6451 CG(orange) and DBSCAN (green).

Appendix A. Spectroscopic Data: APOGEE and GALAH data

Figures A.19 to A.23 show the chemical abundances of members from APOGEE. The upper plots shows members found by Cantat-Gaudin et al. (2018) and the lower ones are our results.

Figures A.24 to A.27 show the chemical abundances of members from GALAH. The upper plot shows members found by (Cantat-Gaudin et al., 2018) and the lower one is our result.

Appendix B. ASteCA plots

Figures B.28 to B.37 show ASteCA plots and CMDs of the revised members that we obtained after running DBSCAN clustering algorithm on our sample.

Table 5: APOGEE and GALAH matches with cluster sample

Cluster	APOGEE	APOGEE	GALAH	GALAH
	CG	DBSCAN	CG	DBSCAN
NGC 2264	71	203	0	0
NGC 2682	430	405	274	279
NGC 2244	191	200	0	0
NGC 3293	25	69	24	88
NGC 6913	60	40	0	0
IC 1805	55	84	0	0
NGC 2243	13	15	8	10
NGC 6451	4	6	0	0
NGC 6583	0	0	23	22



Figure 13: Revised members of NGC 6005 CG(orange) and DBSCAN (green).



Figure 14: Revised members of NGC 6583 CG(orange) and DBSCAN (green).

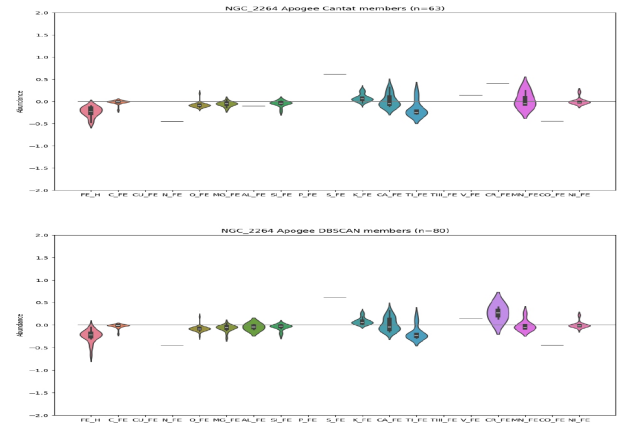


Figure 15: Chemical abundances of members from APOGEE for NGC2264 (a) Upper plot (Cantat-Gaudin et al., 2018) (b) Our results

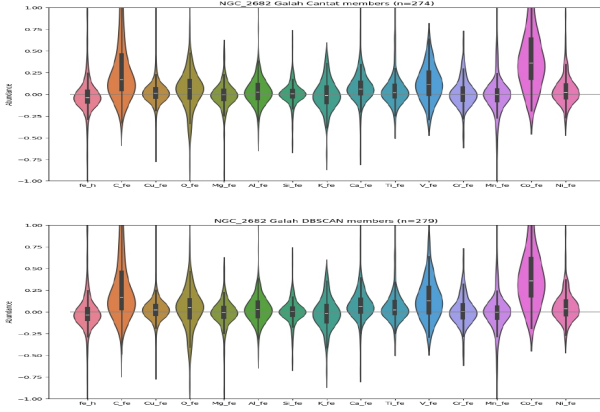


Figure 16: Chemical abundances of members from GALAH for NGC 2682 (a) Upper plot (Cantat-Gaudin et al., 2018) (b) Our results

Cluster	ASteCA log(age)	d	Cantat log(age)	d
NGC 2264	7.176	714	7.44	707
NGC 2682	9.39	1000	9.63	889
NGC 2244	7.34	1061	7.1	1478
NGC 3293	7.4	1459	7.01	2710
NGC 6913	7.8	1318	7.34	1608
NGC 7142	9.6	2238	9.49	2406
IC 1805	7.547	2500	6.88	1964
NGC 6231	7.45	1032	7.14	1475
NGC 2243	9.89	3311	9.64	3719
NGC 6451	7.5	2857	7.41	2777.0
NGC 6005	9.2	2631	9.1	2383.0
NGC 6583	9.0	2439	9.08	2053.0

Table 6: ASteCA Parameters vs parameters from (Cantat-Gaudin and Anders, 2020) using DBSCAN

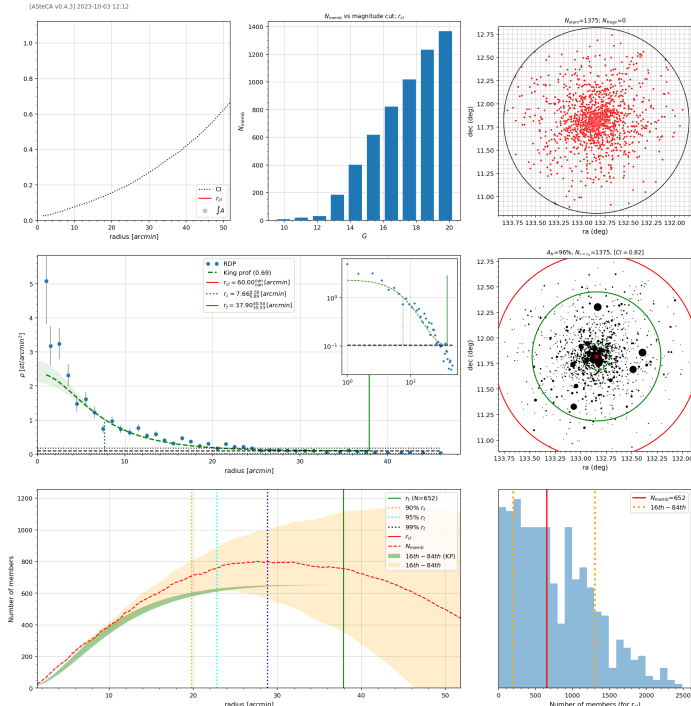


Figure 17: ASteCA plots of NGC 2682

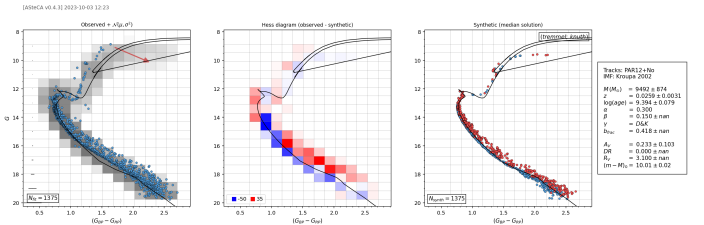


Figure 18: ASteCA CMD plots of NGC 2682

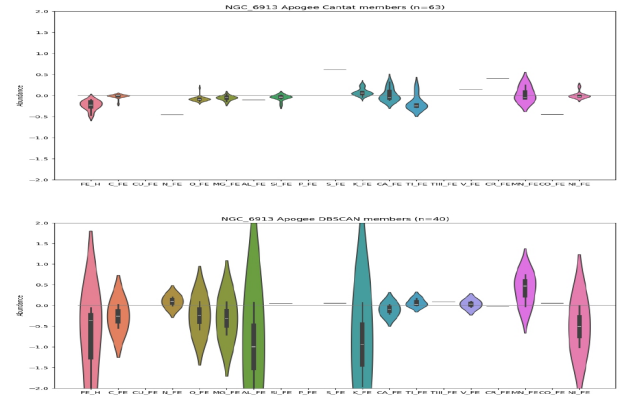
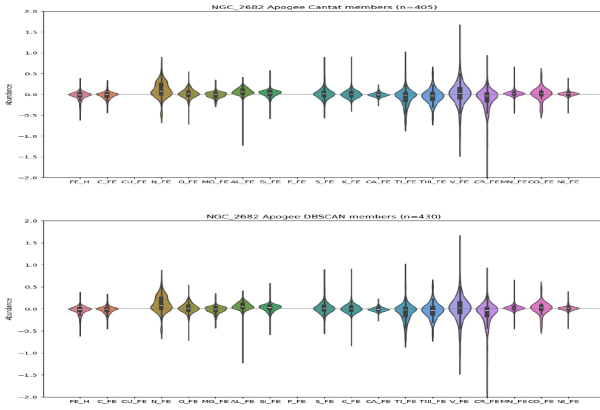


Figure A.19: Chemical abundances of members from APOGEE for NGC 2682
 (a) Upper plot (Cantat-Gaudin et al., 2018) (b) Our results

Figure A.21: Chemical abundances of members from APOGEE for NGC 6913
 (a) Upper plot (Cantat-Gaudin et al., 2018) (b) Our results

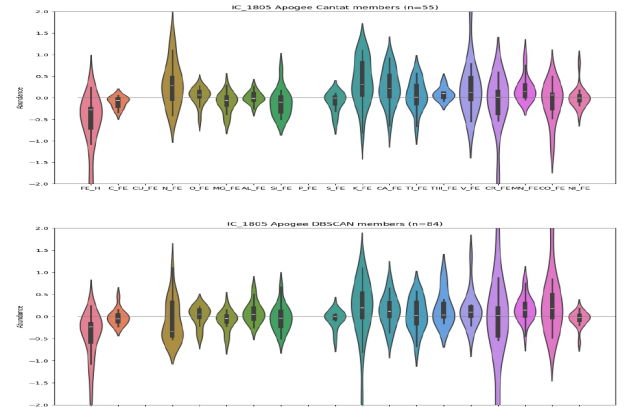
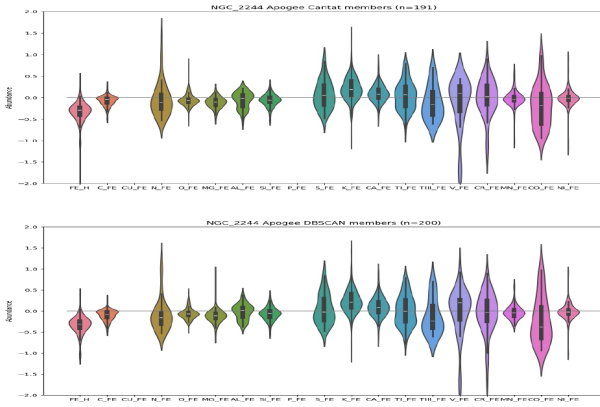


Figure A.20: Chemical abundances of members from APOGEE for NGC 2244
 (a) Upper plot (Cantat-Gaudin et al., 2018) (b) Our results

Figure A.22: Chemical abundances of members from APOGEE for IC 1805
 (a) Upper plot (Cantat-Gaudin et al., 2018) (b) Our results

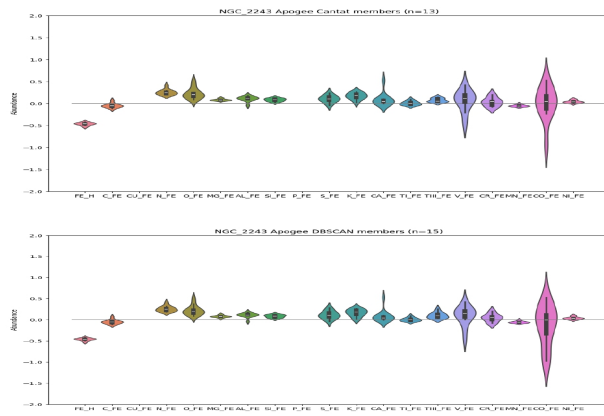


Figure A.23: Chemical abundances of members from APOGEE for NGC 2243
(a) Upper plot (Cantat-Gaudin et al., 2018) (b) Our results

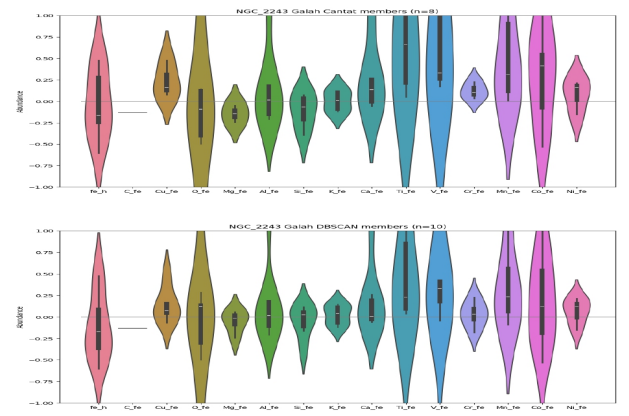


Figure A.25: Chemical abundances of members from GALAH for NGC 2243
(a) Upper plot (Cantat-Gaudin et al., 2018) (b) Our results

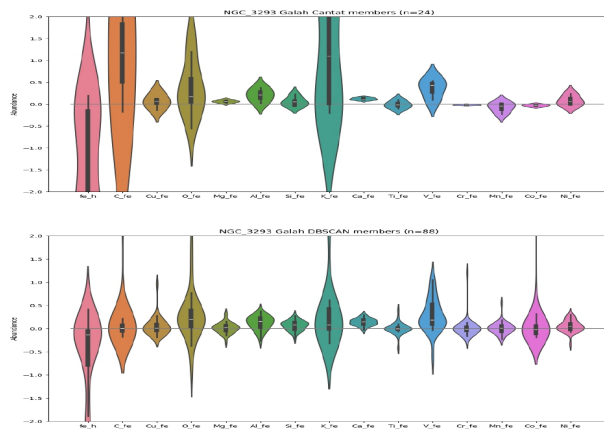


Figure A.24: Chemical abundances of members from GALAH for NGC 3293
(a) Upper plot (Cantat-Gaudin et al., 2018) (b) Our results

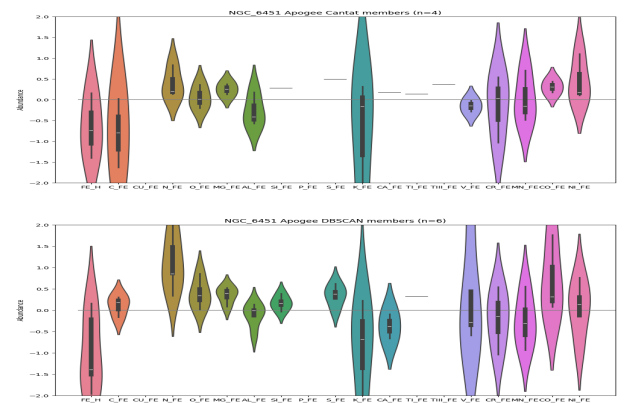


Figure A.26: Chemical abundances of members from GALAH for NGC 6451
(a) Upper plot (Cantat-Gaudin et al., 2018) (b) Our results

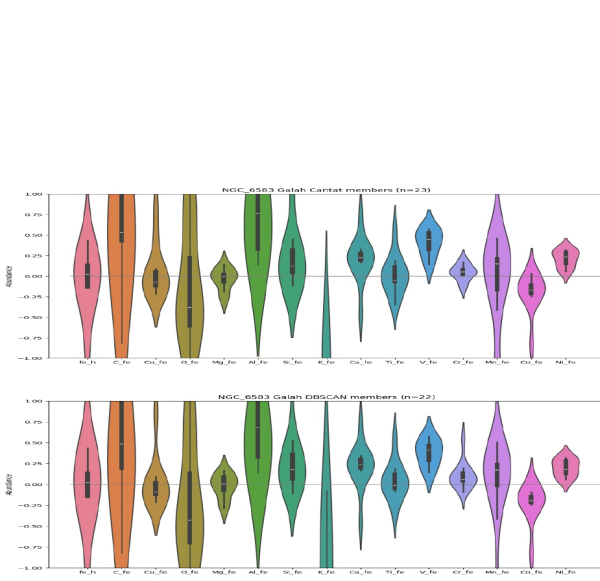


Figure A.27: Chemical abundances of members from GALAH for NGC 6583 (a) Upper plot (Cantat-Gaudin et al., 2018) (b) Our results

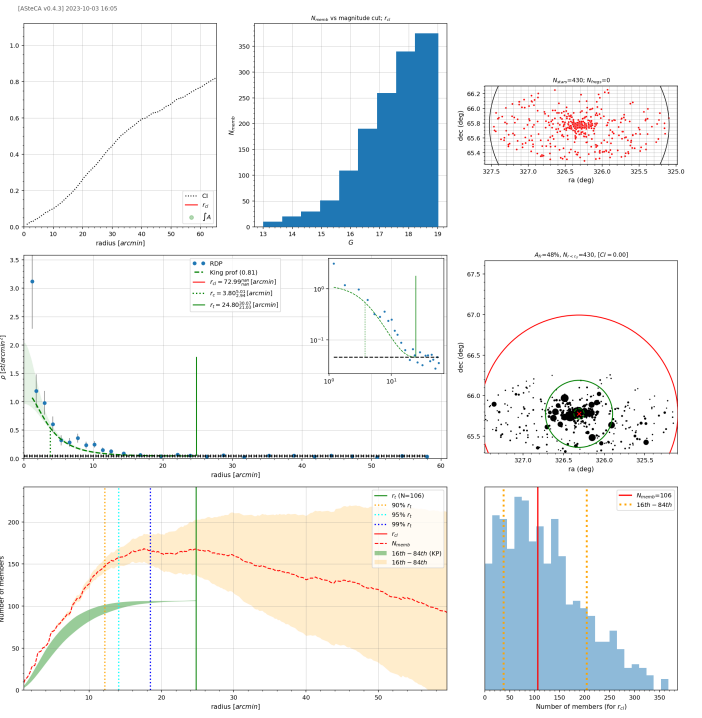


Figure B.29: ASteCA plots of NGC 7142

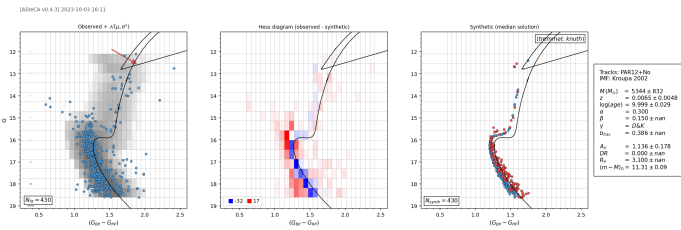


Figure B.28: ASteCA CMD plots of NGC 7142

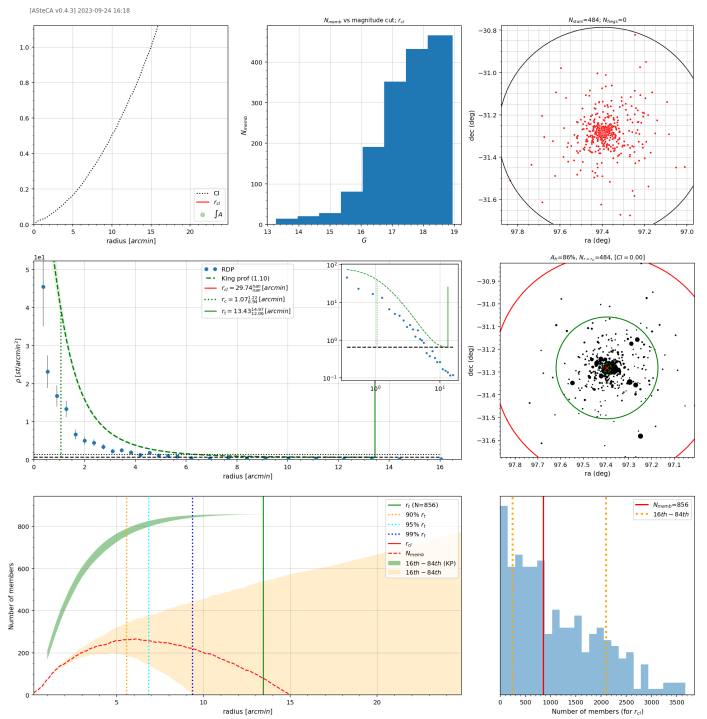


Figure B.30: ASteCA plots of NGC 2243

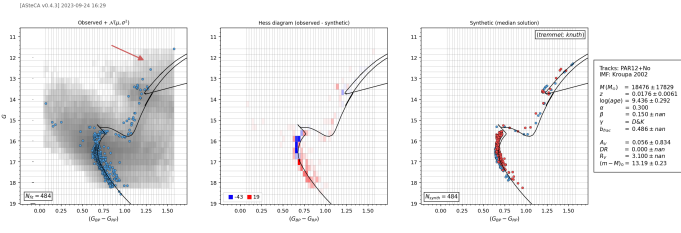


Figure B.31: ASteCA CMD plots of NGC 2243

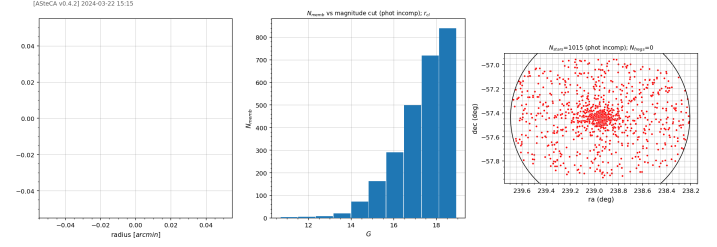


Figure B.34: ASteCA plots of NGC 6005

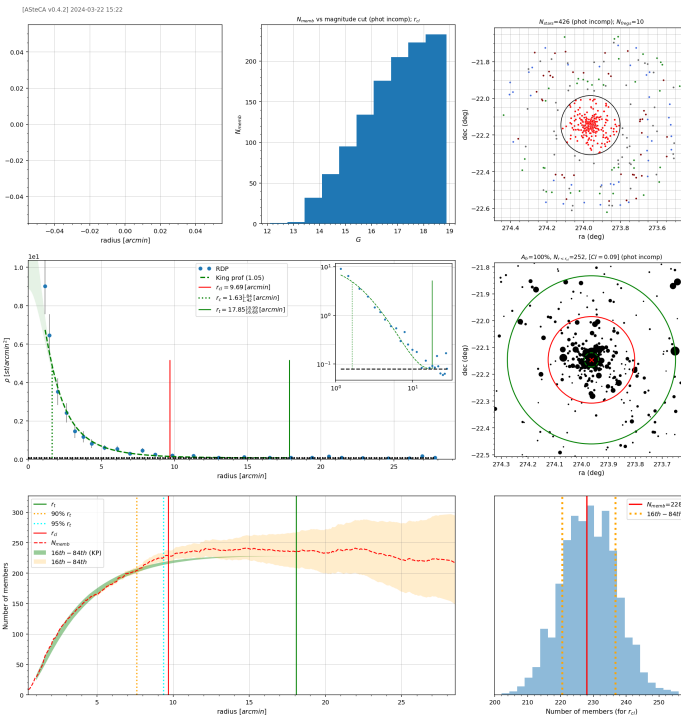


Figure B.32: AsteCA plots of NGC 6451

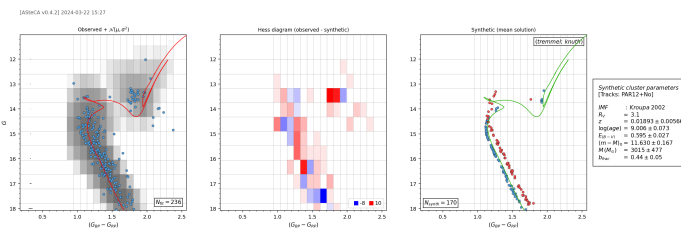


Figure B.33: ASteCA CMD plots of NGC 6451

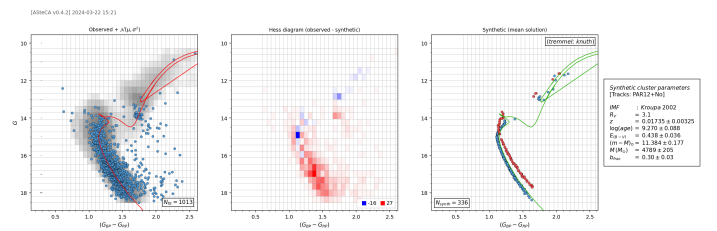


Figure B.35: ASteCA CMD plots of NGC 6005

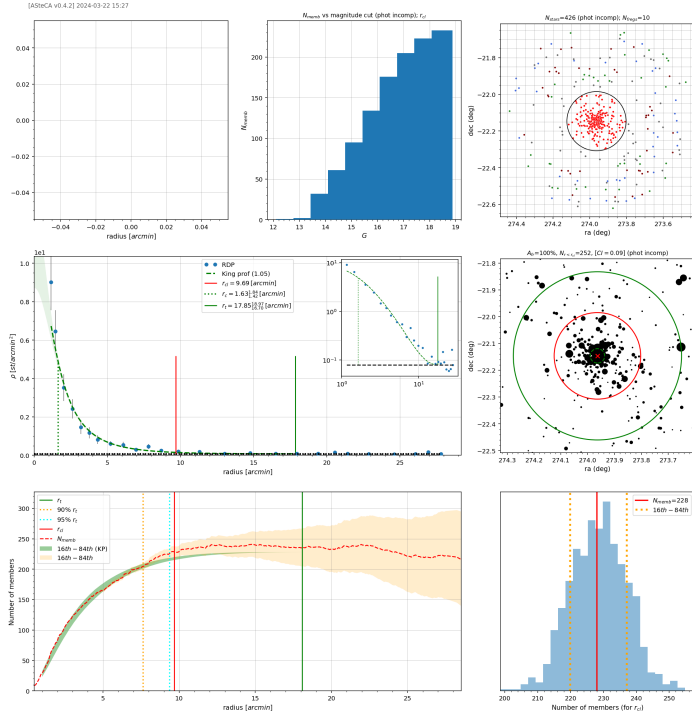


Figure B.36: ASteCA plots of NGC 6583

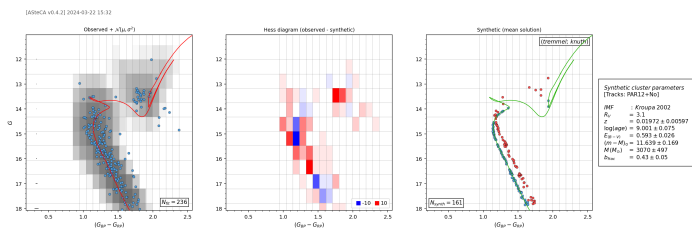


Figure B.37: ASteCA CMD plots of NGC 6583